ELSEVIER

Inorganica Chimica Acta 252 (1996) 141–155

Inorganica Chimica Acta

Methyl-, acetyl- and allyl-palladium and -platinum complexes containing the novel chiral phosphorus-imine 2-(diphenylphosphino)-benzylidene-*S*(−)-α-methyl-benzylamine ligand

Hubertus A. Ankersmit [a], Bjørn H. Løken [b], Huub Kooijman [c], Anthony L. Spek [c,1], Kees Vrieze [a,*], Gerard van Koten [d]

[a] *J.H. van 't Hoff Research Instituut, Laboratorium Anorganische Chemie, Universiteit van Amsterdam, Nieuwe Achtergracht 166, 1018 WV Amsterdam, Netherlands*

[b] *Department of Chemistry, University of Bergen, Allégt. 41, N-5007 Bergen, Norway*

[c] *Bijvoet Centre for Biomolecular Research, Laboratorium Kristal- en Structuurchemie, Universiteit Utrecht, Padualaan 8, 3584 CH Utrecht, Netherlands*

[d] *Debye Institute, Department of Metal-Mediated Synthesis, Universiteit Utrecht, Padualaan 8, 3584 CH Utrecht, Netherlands*

Received 19 March 1996; revised 9 July 1996

Abstract

Neutral compounds of the type $[MX_2(L)]$ and $[MX(Me)(L)]$ and ionic complexes of the type $[M(Me)(L)](O_3SCF_3)$, in which X = Cl, Br, I; M = Pd, Pt; L = 2-(diphenylphosphino)-benzylidene-*S*(−)-α-methyl-benzylamine, have been prepared and characterized. Single crystal X-ray determinations of $[PdCl_2(L)]$ (**1a**) and $[PtI_2(L)]$ (**3b**) showed, in both cases, a chelate coordination of the PN ligand thereby forming a six-membered ring. The square planar surrounding is completed by the two halide atoms. The single crystal X-ray determination of $[PdCl(Me)Cl(L)]$ (**4a**) shows an analogous geometry with a chelating PN ligand, a chloride atom and a methyl group, which is positioned *cis* to the phosphorus atom, completes the square planar surrounding. The methylpalladium and -platinum complexes reacted with CO to give the corresponding acetyl complexes. The insertion rates increased in the order $Cl < Br < O_3SCF_3^-$ while the reaction is first order in metal complex and first order in CO concentration. Complexes $[Pd(\eta^3\text{-allyl})(PN)]^+Y^-$ (Y = Cl, O_3SCF_3) with symmetric allyl groups 2-RC_3H_5 (R = Me, C(O)Me), 2-MeC_3Me_4 and asymmetrically substituted allyl groups 2-R-$C_3H_2Me_2$ (R = H, Me) have been prepared. Temperature dependent ^1H, $^{31}P\{^1H\}$ and $^{13}C\{^1H\}$ NMR has been used to determine the influence of the chiral ligand on the structural aspects and dynamic features. It is shown that a delicate balance between counteracting steric and electronic factors determines the type of isomer, i.e. with the P atom *cis* or *trans* to the CMe_2 moiety of the asymmetric allyl group.

Keywords: Palladium complexes; Imine phosphorus coordination; Insertion reactions; Platinum complexes; Palladium complexes; Chiral ligand complexes

1. Introduction

It has been shown that polyketones, which involve a perfectly alternating array of C–C coupled CO and alkenes, are formed by reactions homogeneously catalyzed by Pd(II) complexes containing *cis*-bidentate diphosphines [1] or *cis*-bidentate nitrogen ligands [2].

Understandably, we are interested in the initial insertion of CO into the Pd–R bond and the subsequent insertion of an alkene in the acylpalladium bond as influenced by the L-L ligand. The L-L ligand may be a symmetric diphosphine [1,3], an asymmetric amino-phosphine [1b] or a bidentate α-diimine ligand, which may be symmetric like R-DAB (R–N=C(H)–C(H)=N–R) [2c], bipy or Ar-BIAN (bis-(arylimino)acenaphthene) [4] or asymmetric like R-Pyca (2-pyridine-carbaldiimine) [2c]. In this context it is of interest to note that van Leeuwen et al. [5] unequivocally showed by using dppp type ligands with slightly different PR_2 units in complexes $[MY(R)(PP')]$ (M = Pt, R = Ph; M = Pd, R = Me; Y = Cl^-, MeOH, CD_2Cl_2) that the so-called insertion of CO involves a migration of the R group to the M bonded CO group.

When considering the role of the L-L ligand we found to our great surprise that, while understandably PP ligands with a flexible backbone and a large bite angle enhance both CO and alkene insertions [1], NN ligands whether flexible or rigid, but both with small bite angles (72–84°) [4], result generally in faster insertions of both CO and norbornadiene.

* Corresponding author.

[1] To whom correspondence should be sent with regards to the crystallographic data.

PII S0020-1693(96)05307-8

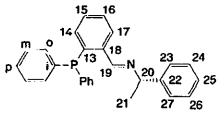

Fig. 1. Schematic structure of the 2-(diphenylphosphino)benzylidene-*S*(−)-α-methyl-benzylamine ligand, with numbering scheme.

Also, the CO insertion rates increase with increasing steric bulk of the substituent close to either N atom of the NN ligand. Perhaps even more surprising is that CO and even the large norbornadiene substrate insert rapidly in $[(terpy)PdMe]^+Y^-$ and $[(terpy)Pd(C(O)Me)]^+Y^-$, respectively [6], begging the question whether or not insertion might occur via five-coordinate intermediates, which are energetically not favored [7].

Relatively little effort has been spent on PN containing complexes, since the CO insertions were relatively slow, while no alkenes could be inserted in the resulting Pd–C(O)R bond. Nonetheless we could show that one of the pathways involved the temporary dissociation of the hard N-donor function of the hemilabile PN ligand [1b].

Here we direct our attention to the synthesis of methylpalladium complexes of a chiral PN ligand with a large backbone and to the study of reactivity of these complexes with CO and allenes. In Fig. 1 the structure of the PN ligand (2-(diphenylphosphino)benzylidene-*S*(−)-α-methyl-benzylamine) is schematically shown.

2. Experimental

2.1. Materials

All reactions were carried out in an atmosphere of purified nitrogen, using standard Schlenk techniques. Solvents were carefully dried and distilled prior to use or stored under an inert atmosphere, unless denoted otherwise. $[PdCl_2(COD)]$, $[PdCl(Me)(COD)]$ [8] (COD = cyclo-1,5-octadiene), $Pd(DBA)_2$ [9] (DBA = dibenzylideneacetone) and 2-diphenylphosphine-benzaldehyde [10] were synthesized by literature procedures. 1-Phenylethylamine, 2-bromobenzaldehyde, 1,2-propadiene (allene), 3-methyl-1,2-butadiene (DMA), 2,4-dimethyl-2,3-pentadiene (TMA), 1-chloro-2-butene and 1-chloro-3-methyl-2-butene are commercially available and were used without further purification.

2.2. Instrumentation

^1H, $^{31}P\{^1H\}$ and $^{13}C\{^1H\}$ spectra were recorded on Bruker AMX 300 and AC 100 spectrometers. Chemical shift values are in ppm relative to Me_4Si (^1H and $^{13}C\{^1H\}$) and 85% H_3PO_4 ($^{31}P\{^1H\}$). Coupling constants are in Hertz (Hz).

Conductivity experiments on **4a** were carried out using a Consort K720 digital conductometer. The CO insertion rates were determined employing a sapphire tube (10.0 mm outer diameter, 8.0 mm inner diameter) [11]. Prior to the NMR experiment, the tube was shaken twice, while connected to the CO pressure line, in order to dissolve CO homogeneously. The CO insertion reaction was monitored by $^{31}P\{^1H\}$ and ^1H NMR at room temperature, employing approximately 0.02 M solutions ($CDCl_3$) of the methylpalladium or -platinum complexes and 10 bar CO, while the chloro-methylpalladium complex was also studied using 5, 10, 15, 17.5, 20, 22.5 and 25 bar CO. Elemental analyses were carried out by Dornis und Kolbe, Muhlheim a.d. Ruhr in Germany.

2.3. Crystal structure determination

Crystals of **1a**, **3b** and **4a**, suitable for X-ray diffraction were glued to the tip of a glass fiber and transferred to an Enraf-Nonius CAD4-T diffractometer on a rotating anode (**3b**) or to an Enraf-Nonius CAD4-F diffractometer with a sealed tube (**1a** and **4a**). Accurate unit-cell parameters and an orientation matrix were determined by least-squares refinement of the setting angles of a number of well-centered reflections (SET4) [12]. The unit-cell parameters were checked for the presence of higher lattice symmetry [13]. Crystal data and details on data collection and refinement are presented in Table 1.

Data were corrected for Lp effects and for the observed linear decay of the reference reflections. For compound **4a** the standard deviations of the intensities as obtained by counting statistics were increased according to an analysis of the excess variance of the reference reflections: $\sigma^2(I) = \sigma^2_{cs}(I) + (0.01I)^2$ [14]. Empirical absorption correction was applied for complexes **1a**, **3b** and **4a** (DIFABS) [15]. F_o values of **1a** were corrected for secondary extinction by refinement of an empirical isotropic parameter: $F'_o = F_c[1 + xF^2c\lambda^3/\sin(2\theta)]^{-1/4}$, with $x = 4.6(5) \times 10^{-6}$. Secondary extinction effects in the reflection data of **4a** were also taken into account by refining an empirical isotropic parameter, using $F'_c = F_c[1 - xF_c^2/\sin\theta]$, with $x = 7.9(7) \times 10^{-7}$.

The structures were solved by automated Patterson methods and subsequent difference Fourier techniques (DIRDIF-92 [16] for **1a**, **4a**; SHELXS86 [17] for **3b**). Compound **4a** was refined on F by full-matrix least-squares techniques (SHELX76) [18]. Complexes **1a** and **3b** were refined on F^2, also using full-matrix least-squares techniques (SHELXL-93) [19]; no observance criterion was applied during refinement of these two structures. Hydrogen atoms were included in the refinement on calculated positions, riding on their carrier atoms. All methyl hydrogen atoms were refined in a rigid group.

The non-hydrogen atoms of all structures were refined with anisotropic thermal parameters. Hydrogen atoms of **4a** were refined with overall isotropic thermal parameter amounting to 0.110(8) Å^2. The hydrogen atoms of the other compounds were refined with fixed isotropic thermal parameter related to the value of the equivalent isotropic thermal parameter of

Table 1
Crystal data of **1a**, **3b** and **4a**

	1a	**3b**	**4a**
Crystal data			
Formula	$C_{27}H_{24}NPCl_2Pd$	$C_{27}H_{24}NPI_2Pt$	$C_{28}H_{27}NPClPd$
Molecular weight	570.79	842.36	550.38
Crystal system	monoclinic	monoclinic	monoclinic
Space group	$P2_1$ (No. 4)	$P2_1$ (No. 4)	$P2_1$ (No. 4)
a (Å)	8.7532(12)	8.6793(6)	8.6893(17)
b (Å)	14.392(3)	15.1383(13)	14.4920(15)
c (Å)	10.475(3)	10.3417(11)	10.542(7)
β (°)	108.49(2)	104.970(7)	71.66(2)
V (Å^3)	1251.5(5)	1312.7(2)	1260.1(7)
D_{calc} (g cm^{-3})	1.515	2.131	1.451
Z	2	2	2
$F(000)$	576	784	560
μ (cm^{-1})	88.7	78.0	7o.o
Crystal size	0.5×0.3×0.2	0.5×0.4×0.3	1.2×0.5×0.4
Data collection			
T (K)	295	150	295
θ_{min}, θ_{max} (°)	3.07, 74.99	1.35, 27.50	3.05, 75.0
SET4 θ_{min}, θ_{max} (°)	16.46, 74.97 (22 refl.)	11.44, 13.97 (24 refl.)	18.08, 23.88 (17 refl.)
Wavelength (Å)	1.54184 (Cu Kα) (Ni filter)	0.71073 (Mo Kα) (graphite monochr.)	1.54184 (Cu Kα) (Ni filter)
Scan type	$\omega/2\theta$	$\omega/2\theta$	$\omega/2\theta$
$\Delta\omega$ (°)	0.69+0.14tanθ	0.66+0.35tanθ	0.53+0.14tanθ
Horizontal, vertical aperture (mm)	3.00, 6.00	2.79, 4.00	3.00, 6.00
X-ray exposure (h)	32	15	66
Linear decay (%)	2	1	<1
Reference reflections	$\bar{2}$ 2 2, 0 2 $\bar{5}$, $\bar{3}$ 0 2	2 5 1, 4 2 0, 3 $\bar{1}$ 2	2 5 1, $\bar{1}$ 5 2, $\bar{4}$ 2 1
Data set	−10:10, 0:18, −13:10	−7:11, 0:19, −13:12	−10:10, −18:−18, −13:13
Total data	4190	4280	10601
Total unique data	2669 (R_{int}=0.045)	3118 (R_{int}=0.044)	5195 (R_{int}=0.068)
Observed data	(no obs. crit. applied)	(no obs. crit. applied)	5171 ($I>2.5\sigma(I)$)
Absorption correction range	0.717, 1.543	0.828, 1.271	0.501, 1.687
Refinement			
No. refined parameters	291	290	290
Final $R1$ [a]	0.037 [2616$F_o>4\sigma(F_o)$]	0.030 [3086$F_o>4\sigma(F_o)$]	0.053
Final w$R2$ [b]	0.094	0.077	
Final R_w [c]			0.062
Goodness of fit	1.06	1.07	1.34
w^{-1} [d]	$\sigma^2(F^2)$+(0.0647P)^2+0.66P	$\sigma^2(F^2)$+(0.0618P)^2+1.51P	$\sigma^2(F)$
$(\Delta/\sigma)_{av}$, $(\Delta/\sigma)_{max}$	0.000, 0.001	0.001, −0.003	0.012, 0.104
Min. and max. residual density (e Å^{-3})	−0.87, 1.16 (near Pd)	−2.57, 2.17 (near Pt)	−1.84, 1.82 (near Pd and Cl)

[a] $R1=\Sigma||F_o|-|F_c||/\Sigma|F_o|$.
[b] $wR2=|\Sigma[w(F_o^2-F_c^2)^2]/\Sigma[w(F_o^2)^2]]^{1/2}$.
[c] $R_w=[\Sigma[w(|F_o|-|F_c|)^2]/\Sigma[w(F_o^2)]]^{1/2}$.
[d] $P=(\max(F_o^2,0)+2F_c^2)/3$.

their carrier atoms by a factor of 1.5 for the methyl hydrogen atoms and 1.2 for the other hydrogen atoms, respectively.

The Flack x parameter [20], derived during the final structure-factor calculation, amounts to 0.004(13) and 0.008(6) for **1a** and **3b**, respectively, indicating correctly assigned absolute structures. Refinement of the alternative chirality of **4a** resulted in the significantly higher R value of 0.076.

Neutral atom scattering factors and anomalous dispersion corrections were taken from the International Tables for Crystallography [21] for **1a** and **3b**. Compound **4a** was refined using neutral atom scattering factors taken from Cromer and Mann [22] amplified with anomalous dispersion corrections from Cromer and Liberman [23]. Geometrical calculations and illustrations were performed with PLATON [24a] and PLUTON [24b], respectively; all calculations were performed on a DECstation 5000. Final coordinates and equivalent isotropic thermal parameters of the non-hydrogen atoms for **1a** and **3b** are given in Table 2, and for **4a** in Table 3.

Table 2
Final coordinates and equivalent isotropic thermal parameters of the non-hydrogen atoms for **1a** and **3b**

1a					**3b**				
Atom	*x*	*y*	*z*	U_{eq}	Atom	*x*	*y*	*z*	U_{eq}
Pd(1)	1.17492(4)	0.49233(3)	0.21152(2)	0.0332(1)	Pt(1)	0.81238(3)	−0.00005(2)	0.77601(2)	0.0110(1)
Cl(1)	0.9775(3)	0.42738(15)	0.0223(1)	0.0689(6)	I(1)	1.03170(6)	−0.06894(4)	0.98210(5)	0.0220(2)
Cl(2)	1.1877(4)	0.35418(13)	0.3202(2)	0.0817(8)	I(2)	0.79582(8)	−0.15267(4)	0.66084(6)	0.0231(2)
P(1)	1.3429(2)	0.55791(9)	0.39343(13)	0.0332(3)	P(1)	0.6524(2)	0.06216(13)	0.5970(2)	0.0114(4)
N(1)	1.1783(6)	0.6151(3)	0.1131(4)	0.0342(12)	N(1)	0.8114(9)	0.1171(5)	0.8760(7)	0.0188(19)
C(1)	1.3775(8)	0.5008(6)	0.5522(6)	0.0492(16)	C(1)	0.6334(9)	0.0098(6)	0.4372(8)	0.0178(19)
C(2)	1.2470(11)	0.4785(8)	0.5952(8)	0.080(4)	C(2)	0.7733(10)	−0.0004(8)	0.3942(8)	0.024(2)
C(3)	1.2713(18)	0.4321(10)	0.7173(10)	0.101(5)	C(3)	0.7665(15)	−0.0457(8)	0.2760(10)	0.034(3)
C(4)	1.420(2)	0.4077(11)	0.7920(11)	0.115(7)	C(4)	0.627(2)	−0.0829(9)	0.2049(11)	0.048(4)
C(5)	1.5535(18)	0.4311(12)	0.7544(11)	0.110(5)	C(5)	0.4902(16)	−0.0735(11)	0.2471(13)	0.047(4)
C(6)	1.5328(11)	0.4774(8)	0.6342(8)	0.072(3)	C(6)	0.4916(14)	−0.0265(8)	0.3602(10)	0.033(3)
C(7)	1.5388(6)	0.5803(4)	0.3755(7)	0.0425(18)	C(7)	0.4528(9)	0.0786(7)	0.6160(9)	0.020(2)
C(8)	1.6045(8)	0.5121(5)	0.3170(8)	0.055(2)	C(8)	0.3820(9)	0.0076(7)	0.6652(9)	0.021(2)
C(9)	1.7553(11)	0.5265(7)	0.3009(12)	0.072(3)	C(9)	0.2315(11)	0.0178(7)	0.6865(11)	0.030(3)
C(10)	1.8359(10)	0.6064(8)	0.3486(15)	0.088(4)	C(10)	0.1558(11)	0.0981(8)	0.6622(13)	0.036(3)
C(11)	1.7737(13)	0.6733(9)	0.409(2)	0.116(7)	C(11)	0.2240(13)	0.1684(9)	0.6166(16)	0.046(4)
C(12)	1.6214(11)	0.6614(6)	0.4242(14)	0.081(4)	C(12)	0.3787(12)	0.1598(8)	0.5945(13)	0.034(3)
C(13)	1.2585(6)	0.6702(4)	0.4099(5)	0.0344(14)	C(13)	0.7297(8)	0.1701(6)	0.5775(8)	0.013(2)
C(14)	1.2643(9)	0.7050(5)	0.5368(6)	0.048(2)	C(14)	0.7191(11)	0.2054(6)	0.4508(9)	0.021(2)
C(15)	1.1983(11)	0.7907(7)	0.5475(8)	0.060(3)	C(15)	0.7882(12)	0.2870(7)	0.4354(9)	0.024(2)
C(16)	1.1294(9)	0.8438(5)	0.4348(8)	0.058(2)	C(16)	0.8624(11)	0.3364(6)	0.5456(9)	0.022(2)
C(17)	1.1243(9)	0.8111(5)	0.3102(8)	0.050(2)	C(17)	0.8690(11)	0.3037(6)	0.6744(9)	0.020(2)
C(18)	1.1868(8)	0.7249(4)	0.2970(6)	0.0368(17)	C(18)	0.8039(9)	0.2209(6)	0.6891(8)	0.0147(19)
C(19)	1.1760(8)	0.6968(4)	0.1587(6)	0.0416(19)	C(19)	0.8120(10)	0.1943(5)	0.8273(9)	0.016(2)
C(20)	1.1785(9)	0.6083(4)	−0.0314(6)	0.0438(19)	C(20)	0.8003(10)	0.1134(6)	1.0194(8)	0.018(2)
C(21)	1.0199(11)	0.6413(7)	−0.1275(8)	0.064(3)	C(21)	0.9483(10)	0.1515(7)	1.1129(9)	0.022(3)
C(22)	1.3280(9)	0.6546(5)	−0.0456(6)	0.0467(19)	C(22)	0.6446(10)	0.1555(6)	1.0315(8)	0.018(2)
C(23)	1.4688(12)	0.6045(8)	−0.0158(12)	0.078(4)	C(23)	0.5060(13)	0.1070(7)	0.9953(11)	0.029(3)
C(24)	1.6087(15)	0.6424(11)	−0.0295(16)	0.105(6)	C(24)	0.3625(13)	0.1429(9)	1.0059(12)	0.036(3)
C(25)	1.6079(15)	0.7314(11)	−0.0753(12)	0.092(5)	C(25)	0.3581(12)	0.2271(8)	1.0554(11)	0.032(3)
C(26)	1.4709(16)	0.7816(7)	−0.1054(9)	0.081(4)	C(26)	0.4959(12)	0.2762(7)	1.0913(9)	0.026(3)
C(27)	1.3304(12)	0.7452(5)	−0.0896(8)	0.060(3)	C(27)	0.6383(10)	0.2403(6)	1.0789(8)	0.020(2)

2.4. Synthesis of the ligand 2-(diphenylphosphino)-benzylidene-S(−)-α-methyl-benzylamine (L)

A mixture of 2-diphenylphosphino-benzaldehyde (5.10 g; 13.0 mmol) and 1-*S*(−)-phenylethylamine (1.57 g; 13.0 mmol) in toluene (25 ml), under a nitrogen atmosphere, was refluxed for 18 h on molsieves [25].

A red oil was obtained after filtration of the molsieves and subsequent evaporation of the solvent under reduced pressure. Purification of the ligand was achieved by column chromatography on silica. Using Et_2O as the eluent caused a yellow band to run, which gave, after evaporation of the solvent, L as a yellow oil in 59% yield ($[\alpha]^{20} = -23.2 \pm 2°$). *Anal.* Found: C, 82.71; H, 6.21; N, 3.59. Calc. for $C_{27}H_{24}NP$: C, 82.42; H, 6.15; N, 3.56%. $^{13}C\{^1H\}$ NMR ($CDCl_3$, 293 K, δ): 24.4 (C^{21}); 69.6 (C^{20}); 126.5 (C^{17}); 128.6 (C^p); 130.0 (C^{15}); 133.0 (C^{16}); 133.8 ([4.5], C^m); 134.0 ([4.5], C^o); 136.5 ([23.3], C^{18}); 137.2 ([27.2], C^i); 139.4 ([16.6], C^{13}); 144.6 (C^{22}); 158.0 ([20.4], C^{19}).

2.5. Synthesis of the complexes

*2.5.1. [$MCl_2(L)$] (M = Pd (**1a**); Pt (**1b**))*

To a stirred suspension of [$PdCl_2$(COD)] (0.16 g; 0.56 mmol) in CH_2Cl_2 (10 ml), a solution of L (0.24 g; 0.62 mmol) in CH_2Cl_2 (15 ml) was added. The mixture was stirred for 18 h at room temperature, after which the solvent was evaporated. The resulting off-white sticky solid was washed with Et_2O (2 × 10 ml) and subsequently dried, which afforded an air stable solid in 95% yield. Slow diffusion of Et_2O into a concentrated solution of **1a** in CH_2Cl_2 afforded yellow crystals. *Anal.* Found: C, 55.89; H, 4.11; N, 2.39. Calc. for $C_{27}H_{24}NPCl_2Pd$: C, 56.82; H, 4.24; N, 2.45%. $^{13}C\{^1H\}$ NMR ($CDCl_3$, 293 K, δ): 22.0 (C^{21}); 70.4 (C^{20}); 133.5 (C^{15}); 134.3 ([11.3], C^{14}); 134.4 (C^{16}); 134.3 (C^m); 136.5 ([8.3], C^o); 138.0 ([15.1], C^i); 139.5(C^{18});.141.5 ([12.8], C^{13}); 141.6 (C^{22}); 162.8 ([9.6], C^{19}).

Compound **1b** was synthesized similarly to **1a**, using [$PtCl_2$(COD)] (0.12 g; 0.32 mmol) in CH_2Cl_2 (10 ml).

Table 3
Final coordinates and equivalent isotropic thermal parameters of the non-hydrogen atoms for **4a**

Atom	x	y	z	U_{eq}
Pd(1)	−0.18377(4)	0.5064	0.21873(4)	0.0348(1)
Cl(1)	0.0071(3)	0.43659(19)	0.03112(19)	0.0768(8)
P(1)	−0.34774(18)	0.57440(13)	0.39671(15)	0.0353(4)
N(1)	−0.1847(6)	0.6327(4)	0.1151(5)	0.0376(16)
C(1)	−0.3856(9)	0.5224(6)	0.5595(7)	0.053(3)
C(2)	−0.2534(11)	0.4976(10)	0.5986(7)	0.078(4)
C(3)	−0.2768(19)	0.4536(9)	0.7204(11)	0.104(5)
C(4)	−0.426(2)	0.4320(11)	0.7973(11)	0.122(7)
C(5)	−0.5576(19)	0.4558(11)	0.7628(11)	0.119(6)
C(6)	−0.5378(12)	0.5035(12)	0.6416(7)	0.093(4)
C(7)	−0.5431(7)	0.5962(5)	0.3820(7)	0.047(2)
C(8)	−0.6124(9)	0.5298(6)	0.3203(8)	0.058(3)
C(9)	−0.7614(11)	0.5433(8)	0.3024(11)	0.080(4)
C(10)	−0.8426(11)	0.6227(10)	0.3446(15)	0.109(6)
C(11)	−0.7795(14)	0.6895(11)	0.404(2)	0.166(11)
C(12)	−0.6278(13)	0.6746(9)	0.4213(16)	0.119(6)
C(13)	−0.2655(7)	0.6883(5)	0.4097(6)	0.0381(17)
C(14)	−0.2712(9)	0.7230(6)	0.5345(7)	0.051(2)
C(15)	−0.2047(11)	0.8091(7)	0.5444(8)	0.056(3)
C(16)	−0.1361(10)	0.861(6)	0.4327(8)	0.058(3)
C(17)	−0.1340(9)	0.8285(6)	0.3092(7)	0.050(2)
C(18)	−0.1929(7)	0.7413(4)	0.2956(6)	0.0347(17)
C(19)	−0.1849(9)	0.7137(5)	0.1595(6)	0.044(2)
C(20)	−0.1857(9)	0.6255(5)	−0.0287(6)	0.049(2)
C(21)	−0.0237(11)	0.6547(7)	−0.1245(7)	0.070(3)
C(22)	−0.3314(11)	0.6731(6)	−0.0450(7)	0.054(3)
C(23)	−0.4758(13)	0.6268(9)	−0.0098(12)	0.084(4)
C(24)	−0.6158(16)	0.6684(13)	−0.0216(14)	0.126(7)
C(25)	−0.6127(18)	0.7539(12)	−0.0674(12)	0.105(6)
C(26)	−0.4722(18)	0.8003(9)	−0.1032(9)	0.092(5)
C(27)	−0.3303(14)	0.7611(7)	−0.0922(8)	0.072(3)
C(28)	−0.1946(9)	0.3795(4)	0.3170(5)	0.0376(18)

Because **1b** is very similar to **1a** no elemental analysis was done.

2.5.2. *[MBr$_2$(L)] (M = Pd (2a); Pt (2b))*

To a suspension of $PdBr_2$ (0.42 g; 0.63 mmol) in CH_2Cl_2 (10 ml) and MeCN (10 ml) a solution of the ligand (0.27 g; 0.69 mmol) in CH_2Cl_2 (5 ml) was added. After 3 h stirring at room temperature a red solution was obtained. Evacuation of the solvents afforded complex **2a** as a red solid in quantitative yield. $^{13}C\{^1H\}$ NMR ($CDCl_3$, 293 K, δ): 21.3 (C^{21}); 71.1 (C^{20}); 132.0 (C^{15}); 132.3 (C^{14}); 132.9 (C^{16}); 133.6 (C^m); 134.3 ([11.3], C^o); 135.0 (C^{18}); 137.3 ([15.1], C^i); 139.5 ([9.1], C^{13}); 139.7 (C^{22}); 161.9 ([18.3], C^{19}). As **2a** is analogous to **2b** no elemental analysis was performed.

Compound **2b** was isolated as an orange solid in 82% yield when the method described for **2a** was used, starting with Na_2PtBr_4 (0.23 g; 0.41 mmol) in MeCN (15 ml). *Anal.* Found: C, 43.01; H, 3.29; N, 1.90. Calc. for $C_{27}H_{24}NPBr_2Pt$: C, 43.33; H, 3.24; N, 1.87%.

2.5.3. *[PtI$_2$(L)] (3b)*

Compound **3b** was prepared similarly to **1a** using [PtI$_2$(COD)] (0.28 g; 0.50 mmol) in CH_2Cl_2 (10 ml). Slow diffusion of Et_2O into a concentrated solution of **3b** in CH_2Cl_2 afforded yellow crystals. *Anal.* Found: C, 38.45; H, 2.92; N, 1.69. Calc. for $C_{27}H_{24}NPI_2Pt$: C, 38.50; H, 2.87; N, 1.66%. $^{13}C\{^1H\}$ NMR ($CDCl_3$, 293 K, δ): 21.8 (C^{21}); 75.2 (C^{20}); 132.5 (C^{15}); 133.8 (C^{14}); 134.1 (C^{16}); 135.2 ([10.6], C^m); 135.9 ([12.4], C^o); 139.4 ([14.5], C^i); 139.8 ([20.6], C^{13}); 139.9 (C^{22}); 160.7 ([5.1], C^{19}).

2.5.4. *[MCl(Me)(L)] (M = Pd (4a); Pt (4b))*

To a stirred solution of [PdCl(Me)(COD)] (0.61 g; 2.30 mmol) in CH_2Cl_2 (10 ml), a solution of L (1.00 g; 2.53 mmol) in CH_2Cl_2 (10 ml) was added. The mixture was stirred for 5 h at room temperature, after which the solvent was evaporated. The resulting yellow sticky solid was washed with Et_2O (2 × 10 ml) and dried, after which a yellow solid, **4a**, was obtained in 92% yield.

A similar reaction of 2-(diphenylphosphino)benzylidene-*R*(+)-α-methyl-benzylamine with [PdCl(Me)(COD)] afforded a yellow solid, which upon slow diffusion of Et_2O into a concentrated solution of *R*(+)-**4a** in CH_2Cl_2 yielded yellow crystals. *Anal.* Found: C, 60.99; H, 4.93; N, 2.61. Calc. for $C_{28}H_{27}NPClPd$: C, 61.11; H, 4.95; N, 2.54%. $^{13}C\{^1H\}$ NMR ($CDCl_3$, 293 K, δ): 3.5 (Pd–CH_3); 22.4 (C^{21}); 66.8 (C^{20}); 127.6 (C^{17}); 129.1 (C^p); 132.4 (C^{15}); 132.7 ([7.5], C^{14}) 132.8 (C^{16}); 133.3 ([9.1], C^m); 135.0 ([13.6], C^{18}); 135.4 ([12.8], C^o); 137.2 ([9.1], C^i); 139.0 ([14.3], C^{13}); 141.9 (C^{22}); 163.0 ([9.1], C^{19}). Complex **4b** was prepared similarly to **4a**, starting from [Pt(Me)-Cl(COD)] (0.286 g; 1.13 mmol). *Anal.* Found: C, 52.66; H, 4.21; N, 2.16. Calc. for $C_{28}H_{27}NPClPt$: C, 52.63; H, 4.26; N, 2.19%. $^{13}C\{^1H\}$ NMR ($CDCl_3$, 293 K) −12.6 ([5.1], Pt–CH_3); 22.0 (C^{21}); 66.7 (C^{20}); 128.3 (C^{17}); 131.8 (C^p); 132.0 (C^{15}); 132.8 ([8.3], C^{14}); 133.7 (C^{16}); 134.6 ([9.7], C^m); 136.0 ([8.3], C^o); 138.5 ([12.8], C^i); 141.6 (C^{22}); 161.2 ([J_{Pt-C} = 9.1], C^{19}).

2.5.5. *[PdBr(Me)(L)] (5a)*

To a solution of **2a** (0.14 g; 0.21 mmol) in CH_2Cl_2 (10 ml) Me_4Sn (0.06 g; 0.32 mmol) was added. The red solution was stirred for 18 h at room temperature in which time the color gradually turned yellow. After evaporation of the solvent a sticky solid was obtained which was washed with Et_2O (2 × 10 ml) and subsequently dried. **5a** was isolated as an orange solid in 85% yield. $^{13}C\{^1H\}$ NMR ($CDCl_3$, 293 K, δ): 0.3 (Pd–CH_3); 20.8 (C^{21}); 66.6 (C^{20}); 127.5 (C^{17}); 128.7 (C^p); 131.7 ([6.0], C^{14}) 133.4 (C^{16}); 133.6 (C^m); 135.5 ([9.1], C^o); 137.5 ([15.5], C^i); 138.2 (C^{13}); 140.2 (C^{22}); 161.4 ([5.3], C^{19}). Elemental analysis failed due to traces of **2a**.

2.5.6. *[MI(Me)(L)] (M = Pd (6a); Pt (6b))*

To a solution of **4a** (0.11 g; 0.20 mmol) in MeOH (10 ml) NH_4I (0.06 g; 0.40 mmol) was added. The color of the solution gradually turned red. After 45 min the solvent was evaporated and the resulting red solid was suspended in CH_2Cl_2 (5 ml). After filtration and subsequent evaporation of the solvent **6a** was obtained in 84% yield as a hygroscopic

red solid. $^{13}C\{^1H\}$ NMR ($CDCl_3$, 293 K, δ): −2.3 (Pd–CH_3); 21.6 (C^{21}); 70.1 (C^{20}); 136.2 ([8.7], C^m); 136.6 ([9.4], C^o); 138.7 ([11.7], C^i); 139.7 ([11.6, C^{13}); 141.8 (C^{22}); 162.3 ([5.8], C^{19}). Complex **6b** was prepared similarly to **6a** starting with **4b** (0.15 g; 0.23 mmol) using 1 week reaction time. $^{13}C\{^1H\}$ NMR ($CDCl_3$, 293 K, δ): −16.7 ([420], Pt–CH_3); 21.7 (C^{21}); 71.9 (C^{20}); 126.1 ([14.6], C^{18}); 128.5 (C^{17}); 129.1 (C^p); 131.8 (C^{15}); 132.0 (C^{14}); 132.8 ([8.4], C^m); 133.5 (C^{16}); 134.5 ([13.1], C^o); 138.8 ([13.1], C^{13}); 141.3 (C^{22}); 161.3 ([J_{Pt-C} = 10.0, C^{19}). Elemental analysis of **6a** (and **6b**) failed due to small amounts of solvent and NH_4I in the product.

2.5.7. [M(Me)(L)](O$_3$SCF$_3$) (M = Pd (7a); Pt (7b))

To a solution of **4a** (0.14 g; 0.25 mmol) in MeOH (15 ml) $Ag(O_3SCF_3)$ (0.07 g; 0.27 mmol) was added. After 15 min the resulting suspension was filtered and the solvent was subsequently evaporated resulting in an instable off-white solid **7a** in 95% yield. ^{13}C NMR (CD_3OD, 293 K, δ): 4.7 (Pd–CH_3); 20.8 (C^{21}); 66.6 (C^{20}); 129.8 (C^{17}); 132.5 (C^p); 132.7 (C^{15}); 133.4 (C^{16}); 133.5 ([8.0], C^{14}); 134.3 ([9.0], C^m); 134.7 ([9.9], C^{18}); 134.9 (C^o); 137.8 ([3.8], C^i); 137.9 ([9.0], C^{13}); 141.3 (C^{22}); 163.1 ([5.0], C^{19}). Complex **7b** was prepared in situ, similar to **4a**, using **4b** (0.05 g; 0.08 mmol) in $CDCl_3$ (0.8 ml). Elemental analysis of **7a** and **7b** could not be carried out due to slow degradation of the solid product, with formation of colloidal palladium or platinum.

2.5.8. [Pd{η^3-C(R^{1syn})(R^{1anti})C(R^2)C(R^{3syn})(R^{3anti})}(L)][Cl] (R^2 = H, R^{1syn} = R^{1anti} = Me, R^{3syn} = R^{3anti} = H (8a))

To a solution of $Pd(DBA)_2$ (0.24 g; 0.45 mmol) in CH_2Cl_2 (5 ml), 1-chloro-3-methyl-2-butene (0.05 g; 0.45 mmol) and L (0.17 g; 0.45 mmol) in CH_2Cl_2 (5 ml) were added. The purple solution was stirred at room temperature and turned yellow after 45 min. After evaporation of the solvent an orange solid was obtained which was suspended in hexane (40 ml). After filtration, evaporation of the hexane and drying in vacuo, yellow complex **8a** was isolated in 78% yield. $^{13}C\{^1H\}$ NMR ($CDCl_3$, 223 K, δ): allyl unit: 21.2 (broad, Me^{anti}); 27.0 (broad, Me^{syn}); 54.2 (broad, C^3); 106.7 (broad, C^2H); relevant ligand resonances: 14.4 (broad, C^{21}); 70.1 (broad, C^{20}); 164.1 (broad, C^{19}). Complex **8a** showed a specific conductivity of Δ = 98 Ω^{-1} cm^2 mol^{-1} (CH_2Cl_2, 293 K); Δ = 3134 Ω^{-1} cm^2 mol^{-1} (CH_3OH, 293 K). Elemental analyses of **8a** failed due to the presence of 1-chloro-3-methyl-2-butene in the product.

2.5.9. [Pd{η^3-C(R^{1syn})(R^{1anti})C(R^2)C(R^{3syn})(R^{3anti})(L)}][Cl] (R^2 = Me, R^{1syn} = R^{1anti} = R^{3syn} = R^{3anti} = H (9a); R^2 = C(O)Me, R^{1syn} = R^{1anti} = R^{3syn} = R^{3anti} = H (10a); R^2 = Me, R^{1syn} = R^{1anti} = H R^{3syn} = R^{3anti} = Me (11a); R^2 = Me, R^{1syn} = R^{1anti} = R^{3syn} = R^{3anti} = Me (12a))

To a stirred solution of [(PdCl(η^3-$CH_2C(Me)CH_2$)]$_2$ [26] (0.10 g; 0.26 mmol) in CH_2Cl_2 (4 ml) at room temperature a solution of L (0.21 g; 0.53 mmol) in CH_2Cl_2 (3 ml) was added. The mixture was stirred for 1 h after which the solvent was removed in vacuo, yielding **9a** as a yellow solid. **9a**: $^{13}C\{^1H\}$ NMR ($CDCl_3$, 313 K, δ): allyl unit: 20.8 (broad, C^2Me); 59.7 (broad, C^1H_2); 127.5 (broad, C^2); ligand: 22.4 (broad, C^{21}); 72.8 (broad, C^{20}); 167.1 (broad, C^{19}). $^{13}C\{^1H\}$ NMR ($CDCl_3$, 213 K, δ): allyl unit: 18.8, 22.2 ($C^3(Me)H$); 60.0, 54.0 (C^1H_2); 122.3, 123.3 (C^2); relevant ligand resonances: 23.0, 22.0 (C^{21}); 72.6, 73.8 (C^{20}); 168.2 (broad, C^{19}). Complex **9a** showed a specific conductivity of Δ = 159 Ω^{-1} cm^2 mol^{-1} (CH_2Cl_2, 293 K); Δ = 3529 Ω^{-1} cm^2 mol^{-1} (MeOH, 293 K).

Complexes **10a**, **11a** and **12a** were obtained via the same procedure starting from [PdCl{η^3-$CH_2C(C(O)Me)CH_2$}]$_2$, [PdCl{η^3-$CH_2C(Me)C(Me)_2$}]$_2$ and [PdCl{η^3-$C(Me)_2C(Me)C(Me)_2$}]$_2$ respectively. **10a**: $^{13}C\{^1H\}$ NMR ($CDCl_3$, 293 K, δ): allyl unit: 26.8, 26.3 ($C(O)Me$); 50.5 ($C^{trans\text{-}N}$); 61.0 (broad, $C^{trans\text{-}P}$); 137.8 (C^2); relevant ligand resonances: 21.6 (C^{21}); 70.1 (C^{20}); 163.8 (C^{19}). **11a**: $^{13}C\{^1H\}$ NMR ($CDCl_3$, 293 K, δ): allyl unit: 20.7 (broad, Me^{anti}); 21.6 (broad, C^2Me); 26.8 (broad, Me^{syn}); 62 (broad, C^3H_2); 107.8 (broad, C^2); 189.2 (broad, C^1); relevant ligand resonances: 14.4 (broad, C^{21}); 70.1 (broad, C^{20}); 162.3 (broad, C^{19}). Complex **11a** showed a specific conductivity of Δ = 138 Ω^{-1} cm^2 mol^{-1} (CH_2Cl_2, 293 K); Δ = 3422 Ω^{-1} cm^2 mol^{-1} (MeOH, 293 K). **12a**: $^{13}C\{^1H\}$ NMR ($CDCl_3$, 293 K, δ): allyl unit: 15.1 (Me^2); 17.5 (broad, Me$^{trans\text{-}P,\ anti}$); 21.6 (Me$^{trans\text{-}N,\ anti}$); 24.3 (broad, Me$^{trans\text{-}P,\ syn}$); 24.5 (Me$^{trans\text{-}N,\ syn}$); 117.0 (broad, C^2); 126.9 ($C^{trans\text{-}P}$); relevant ligand resonances: 22.1 (broad, C^{21}); 63.4 (C^{20}); 162 (broad, C^{19}). Complex **12a** showed a specific conductivity of Δ = 3628 Ω^{-1} cm^2 mol^{-1} (MeOH, 293 K); Δ = 4819 Ω^{-1} cm^2 mol^{-1} (MeOH, 313 K).

2.5.10. [Pd{η^3-C(R^{1syn})(R^{1anti})C(R^2)C(R^{3syn})(R^{3anti})}(L)]-(O$_3$SCF$_3$) (R^2 = H, R^{1syn} = R^{1anti} = Me, R^{3syn} = R^{3anti} = H (13a); R^2 = Me, R^{1syn} = R^{1anti} = H, R^{3syn} = R^{3anti} = Me (14a))

To a stirred solution of **8a** (0.09 g; 0.16 mmol) in $CDCl_3$ (5 ml) $Ag(O_3SCF_3)$ (0.04 g; 0.17 mmol) was added, resulting in the formation of a white precipitate, which was filtered off, yielding **13a**. Complex **14a** was made via the same procedure starting from **9a** and **11a**, respectively. Isolation of **13a** and **14a** caused slow degradation of the yellow solid with the formation of colloidal palladium. Complex **13a** showed a specific conductivity of Δ = 3984 Ω^{-1} cm^2 mol^{-1} (MeOH, 293 K).

2.5.11. [MX(COMe)(L)] (M = Pd: X = Cl (15a); X = Br (16a); X = I (17a); X = O$_3$SCF$_3$ (18a); M = Pt: X = Cl (15b); X = I (17b); X = O$_3$SCF$_3$ (18b))

In a typical experiment complex **4a** (approximately 0.15 mmol) in $CDCl_3$ (1.5 ml) was pressurized with CO (10 bar) at room temperature in a high-pressure 10 mm NMR tube. The product **15a** was purified by filtration of the solution over celite. Elemental analysis could not be performed due to

gradual degradation of the product with formation of colloidal palladium. **15a**: IR (CH_2Cl_2, cm^{-1}): 1712 (C=O). $^{13}C\{^1H\}$ NMR ($CDCl_3$, 293 K, δ): 21.5 (C^{21}); 39.6 ([23.4], Pd–C(O)CH_3); 65.5 (C^{20}); 131.8 (C^{17}); 132.1 (C^p); 132.5 ([6.8], C^{15}); 134.2 ([12.0], C^{14}); 134.4 (C^{16}); 134.5 ([12.8], C^m); 130.0 ([35.5], C^i); 137.0 ([9.1], C^o); 137.7 ([13.6], C^{13}); 140.8 (C^{22}); 164.1(C^{19}). Complexes **16a**, **17a**, **18a**, **15b**, **17b** and **18b** were synthesized similarly to **15a**, starting from **5a**, **6a**, **7a**, **4b**, **6b** and **7b**, respectively. Elemental analyses could not be performed due to gradual degradation of the products with formation of colloidal palladium (**16a**, **17a** and **18a**) or platinum (**15b**, **16b**, **17b** and **18b**). **16a**: IR (CH_2Cl_2, cm^{-1}): 1705 (C=O). $^{13}C\{^1H\}$ NMR ($CDCl_3$, 293 K, δ): 20.7 (C^{21}); 40.3 ([23.3], Pd–C(O)CH_3); 65.7 (C^{20}); 127.6 (C^{17}); 131.0 (C^p); 131.2 (C^{15}); 131.6 ([6.8], C^{14}); 132.3 (C^{16}); 133.2 ([17.4], C^m); 136.1 ([9.1], C^o); 136.9 ([13.6], C^{18}); 138.3 (C^i); 138.8 (C^{13}); 139.9 (C^{22}); 163.5 (C^{19}). **17a**: IR (CH_2Cl_2, cm^{-1}): 1712 (C=O). $^{13}C\{^1H\}$ NMR ($CDCl_3$, 293 K, δ): 20.8 (C^{21}); 43.5 ([24.2], Pd–C(O)CH_3); 68.0 (C^{20}); 127.7 (C^{17}); 131.0 (C^p); 131.2 (C^{15}); 131.6 ([6.8], C^{14}); 133.6 (C^{16}); 133.7 ([12.8], C^m); 136.0 ([9.1], C^o); 137.1 ([9.1], C^i); 139.7 ([12.8], C^{13}); 139.8 (C^{22}); 163.7 (C^{19}). 226.6 ([9.1], C(O)Me). **18a**: IR (CH_2Cl_2, cm^{-1}): 1715 (C=O). **15b**: IR (CH_2Cl_2, cm^{-1}): 1687 (C=O). **16b**: IR (CH_2Cl_2, cm^{-1}): 1691 (C=O). **17b**: IR (CH_2Cl_2, cm^{-1}): 1685 (C=O). **18b**: IR (CH_2Cl_2, cm^{-1}): 2109 (Pt–C(O) *trans* to P).

3. Results

The yellow bidentate PN ligand (L) shows phosphorus coupling of 4.6 Hz on the imine proton of the free ligand, observed in the ^1H NMR, which points to a through-space coupling [27], indicating that the imine H atom (H^{19}) is directed towards the lone pair of the phosphorus atom.

Neither the ligand L nor the complexes, except for the acyl products, could be properly studied by IR owing to overlap of the imine stretch vibrations by phenyl absorptions. Also Raman spectra could not be measured due to fluorescence phenomena.

The neutral bis-halide complexes [MX_2(L)] (X = Cl (**1**), Br (**2**), I (**3**)) were made by reaction of [MCl_2(COD)], $PdBr_2$, Na_2PtBr_4 or [PtI_2(COD)] with the PN ligand. The methyl complexes [MCl(Me)(L)] (**4**) were prepared by reaction of the PN ligand with [MCl(Me)(COD)], whereas the [PdBr(Me)(L)] complex (**5**) was obtained by reacting [$PdBr_2$(L)] with Me_4Sn. The corresponding methyl-iodide complexes (**6**) were prepared by reacting [MCl(Me)(L)] with NH_4I. The ionic complexes [M(Me)(L)]O_3SCF_3 (**7**) were formed by abstracting the halide ligand from [MCl(Me)(L)] with $Ag(O_3SCF_3)$ (Scheme 1). The palladium complexes are labeled **a** and the corresponding platinum compounds **b**.

The neutral complexes **1a–6a** and **1b–6b** dissolve in polar solvents and can be stored in the open air for a prolonged period. Heating solutions of complexes **1a–6a** and **1b–6b** in CH_2Cl_2 or $CDCl_3$ ($T > 363$ K, 18 h), caused slow decomposition as shown by the formation of traces of colloidal palladium and platinum. The ionic complexes (**7**) are very hygroscopic and unstable and were therefore prepared in situ.

3.1. [MX_2(L)] (1a–3a, 1b–3b); [MX(Me)(L)] (4a–7a, 4b–7b)

The molecular structures of **1a** and **3b** in the solid state (Fig. 2) show the expected square planar coordination around the metal center formed by the P (Pd–P = 2.2144(16) Å (**1a**); 2.217(2) Å (**3b**)) and N (Pd–N = 2.051(4) Å (**1a**); 2.054(7) Å (**3b**)) donor atoms of the chelating ligand

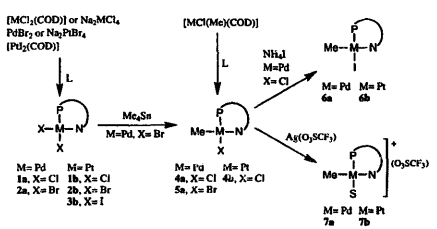

Scheme 1. Numbering of the starting complexes and products.

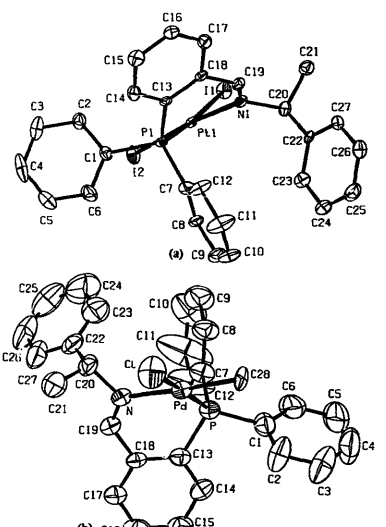

Fig. 2. Crystal structures of (a) [PtI_2(L)] (**3b**) and (b) [PdCl(Me)(L)] (**4a**). ORTEP drawings are drawn with 50% probability level; hydrogens are omitted for clarity.

Table 4
Selected distances (Å) and angles (°) of **1a**, **3b** and **4a**

1a		3b		4a	
Pd–Cl1	2.370(2)	Pt–I1	2.6754(6)	Pd–Cl1	2.371(3)
Pd–Cl2	2.276(2)	Pt–I2	2.5863(7)	Pd–C28	2.098(6)
Pd–P1	2.2144(16)	Pt–P1	2.217(2)	Pd–P1	2.200(2)
Pd–N1	2.051(4)	Pt–N1	2.054(7)	Pd–N1	2.133(6)
Cl1–Pd–C12	88.90(8)	I1–Pt–I2	87.83(2)	Cl1–Pd–C28	87.06(17)
C12–Pd–P1	91.64(7)	I2–Pt–P1	92.67(5)	C28–Pd–P1	93.16(16)
P1–Pd–N1	87.36(13)	P1–Pt–N1	88.3(2)	P1–Pd–N1	86.94(15)
N1–Pd–Cl1	92.39(13)	N1–Pt–I1	91.7(2)	N1–Pd–Cl1	93.06(15)
P1–Pd1–N1–C19	−40.7(6)	P1–Pt1–N1–C19	−37.7(8)	P1–Pd1–N1–C19	38.0(6)
Pd1–N1–C19–C18	6.7(11)	Pt1–N1–C19–C18	4.1(14)	Pd1–N1–C19–C18	−3.4(11)
N1–C19–C18–C13	24.3(12)	N1–C19–C18–C13	27.7(15)	N1–C19–C18–C13	−27.2(12)
C19–C18–C13–P1	−0.7(9)	C19–C18–C13–P1	−5.4(11)	C19–C18–C13–P1	3.7(9)

Table 5
$^{31}P\{^1H\}$ and relevant ^1H NMR data of complexes **1a–7b** and **15a–18b**

No. [Solvent]	$^{31}P\{^1H\}$	H^{19}	H^{20} [a]	H^{21}	Pd–Me	Pd–COMe
L	−12.2	9.11[d][4.6]	1.50[d]	4.55[q]		
(1a) [$CDCl_3$]	32.2	7.75[s]	1.53[d]	6.73[q]		
(2a) [$CDCl_3$]	33.5	7.76[s]	1.53[d]	6.68[b]		
(4a) [$CDCl_3$]	38.2	7.87[s]	1.53[d]	6.56[q]	0.64[d][2.9]	
(5a) [$CDCl_3$]	37.9	7.82[s]	1.49[d]	6.60[q]	0.71[d][3.3]	
(6a) [$CDCl_3$]	34.4	7.80[s]	1.50[d]	6.58[q]	0.77[b]	
(7a) [CD_3OD]	41.6	8.55[s]	1.65[d]	5.49[q]	0.32[s]	
(15a) [$CDCl_3$]	20.3	7.93[s]	1.59[d]	5.61[q]		2.19[s]
(16a) [$CDCl_3$]	19.1	7.77[3.2]	1.49[d]	6.33[q]		2.32[s]
(17a) [$CDCl_3$]	16.5	7.70[3.0]	1.46[d]	6.37[q]		2.35[s]
(18a) [CD_3OD]	24.2	7.89[1.9]	1.58[d]	5.64[q]		2.19[s]
(1b) [$CDCl_3$]	6.2{3771}	8.00{105}	1.52[d]	7.00[q]		
(2b) [$CDCl_3$]	6.1{3710}	8.02{107}	1.51[d]	6.96[q]		
(3b) [$CDCl_3$]	9.4{3471}	7.80{100}	1.47[d]	7.02[q]		
(4b) [$CDCl_3$]	16.7{4714}	8.10{37}	1.56[d]	7.02[q]	0.64{72}[3.5]	
(6b) [$CDCl_3$]	18.1{4552}	7.97{38}	1.47[d]	6.98[q]	0.89{75}[4.5]	
(7b) [$CDCl_3$]	11.3{5335}	8.34{41}	1.66[d]	6.00[b]	0.60{63}[b]	
(15b) [$CDCl_3$]	7.71{4976}	7.85{32}	1.52[d]	6.60[q]		2.12[s]
(17b) [$CDCl_3$]	7.35{4845}	7.72{29}	1.45[d]	6.75[q]		2.15[s]
(18b) [$CDCl_3$]	12.4{3965}	7.95{31}	1.51[d]	6.62[q]		2.02[s]

Coupling constants $^1J_{Pt-P}$, $^3J_{Pt-H}$[a] are given given between { }. Coupling constants J_{P-H} are given between [ ]. [b] broad, [d] doublet, [q] quintet of which the coupling constants could not be properly determined.
[a] 4.5 Hz < $^3J(H^{21}–H^{20})$ > 6.9 Hz.

and two chloride atoms (**2a**, Pd–Cl1 = 2.370(2) Å; Pd–Cl2 = 2.276(2) Å) or two iodide atoms (**3b**, Pt–I1 = 2.6754(6) Å; Pt–I2 = 2.5863(7) Å). All these distances (Table 4) are in the normal range [28]. The dihedral angles of −0.7(9)°, observed in the solid state structure of **1a**, for C19–C18–C13–P1 and −40.0(5)° for the Pd–P1–C13–C18 units, respectively, point to a perturbed envelope configuration of the six-membered ring, in which C20 has an *S* configuration, resulting in an axially positioned α-phenyl-ethyl moiety in the chelate ring, which is also observed for **3b**.

In solution coordination of the phosphorus donor atom is clear from the downfield shift of the $^{31}P\{^1H\}$ NMR resonance signal (Table 5), compared to the free ligand, which is approximately 40 ppm for the bis-halide palladium complexes and 18 ppm for the corresponding platinum compounds. The latter complexes show a platinum–phosphorous coupling which decreases going from chloride ($^1J_{Pt-P}$ = 3771 Hz) to iodide ($^1J_{Pt-P}$ = 3471 Hz) owing to the *trans* influence of the halide [29]. The disappearance of the through-space phosphorus-imine proton coupling ^1H NMR (Table 5) of the bis-halide complexes, indicates a rotation of the C18–C19 bond as is needed for chelate bonding. Coordination of the imino nitrogen donor is also highlighted by the upfield shift of the imine hydrogen atom (Δδ = 1.4 ppm for Pd; Δδ = 1.1 for Pt) and the ^{195}Pt coupling on the imine H atom ($^3J_{Pt-H}$ = 105 Hz (**1b**); 107 Hz (**2b**); 100 Hz (**3b**)). This is also

consistent with the $^{13}C\{^1H\}$ NMR data for **1a**, **2a** and **3b** (Section 2) which show a downfield shift of the C19 and C20 resonance signals of approximately 2 ppm and a phosphorus coupling on the C19 signal of approximately 9.5 Hz.

In order to study the ligand geometry of the opposite configuration in the complex 2-(diphenylphosphino)-benzylidene-*R*(+)-α-methyl-benzylamine was reacted with [PdCl(Me)(COD)] resulting in *R*(+)-**4a**, which shows, as expected, the same coordination features of the ligand towards the palladium center (Pd–P = 2.200(2) Å; Pd–N = 2.133(6) Å) in the solid state, as in structures **1a** and **3b** (Fig. 2), although C20 has an *R* configuration contrary to **1a** and **3b**. Substitution of one of the halides by a methyl group (Pd–C28 = 2.098(6) Å) does not alter the geometry of the chelating ligand. The methyl group is positioned *cis* to the phosphine function, as was expected [1b,30], while the chloride is bonded *trans* to the phosphine donor (Pd–Cl = 2.371(3) Å). When comparing the Pd–N bond of **1a** (2.05 Å) with this bond in **4a** (2.13 Å) an elongation, due to the larger *trans* influence of the methyl group compared to the chloride ligand [30], is observed.

The methylpalladium complexes (**4a–6a**) show a downfield shift in the $^{31}P\{^1H\}$ NMR spectra (Table 5) of approximately 5 ppm, compared to the bis-halide complexes, indicating phosphorus coordination. N bonding of the ligand is further demonstrated by the upfield ^1H NMR shift (Table 5) of the imine proton resonance ($\Delta\delta = 1.31–0.56$ ppm), when compared to the free ligand. In the $^{31}P\{^1H\}$ NMR spectra of the platinum complexes (**4b** and **6b**), large $^{195}Pt–^{31}P\{^1H\}$ couplings of 4714 Hz (**4b**) and 4552 Hz (**6b**) are present, while the ^1H NMR spectra show $^{195}Pt–^1H$ coupling constants of 72 Hz (**4b**) and 75 Hz (**6b**) on the methyl group and 37 Hz (**4b**) and 38 Hz (**6b**) on the imine proton resonance. In the $^{13}C\{^1H\}$ NMR spectrum of **6b** a $^{195}Pt–^{13}C$ coupling constant of 420 Hz on the Pt–Me group is observed. These results are in accord with the bidentate coordination mode of the ligand with the methyl group again *cis* to the phosphorus donor atom [1b].

The OTf anion in complexes **7a** and **7b** was found to be non-coordinating in solution, as shown by the ^{19}F NMR resonance shift of −78.4 ppm (**7a**) and −78.2 ppm (**7b**) [31]. The bidentate PN-coordination mode of the ligand is clear from the downfield shift of the $^{31}P\{^1H\}$ resonance ($\Delta\delta = 3.4$ ppm) and the downfield shift of the imine proton in ^1H NMR ($\Delta\delta = 0.7$ ppm) compared to [PdCl(Me)(L)], whereas the platinum analogue shows an upfield shift in the $^{31}P\{^1H\}$ NMR spectra ($\Delta\delta = 5.4$ ppm) with a large platinum phosphorus coupling of 5335 Hz, while the Pt–H coupling constant of 41 Hz on the imine proton and the upfield shift in ^1H NMR ($\Delta\delta = 0.8$ ppm), compared to the free ligand, indicates nitrogen coordination (Table 5).

3.2. *[Pd{η³-allyl}(L)][X] (X = Cl, OTf) (8a–14a)*

Recently reported insertions of (substituted) allenes into the methylpalladium bond of [PdX(Me)(N-N)] [32,33] prompted us to study the insertion of allenes into the Pd–R bond of [PdX(Me)(PN)] complexes. Since these insertions were found to proceed very slowly (after two weeks only 60% of **7a** was converted to **13a**) and since we are interested in the structural features of allylpalladium complexes with the chiral PN ligand in comparison with the N–S complexes [34], we decided to prepare [Pd{η³-allyl}(L)][X] complexes via alternative routes (Scheme 2). Complex [Pd{η³-allyl}(L)][Cl] with a proton on the central carbon atom (**8a**) was made by reacting $Pd(DBA)_2$ with (substituted)chlorobutene in the presence of L, while the analogous methyl and acyl substituted allyl complexes (**9a–12a**) were obtained by reacting L with $[PdX(\eta^3\text{-allyl})]_2$, complexes with X = OTf (**13a** and **14a**) were obtained by reaction of [Pd{η³-allyl}(L)][Cl] with AgOTf.

The downfield $^{31}P\{^1H\}$ NMR resonance shifts ($30 < \Delta\delta\ ^{31}P\{^1H\} < 40$ ppm) and the upfield shift of the ^1H imine proton ($0.01 < \Delta\delta\ ^1H < 0.73$ ppm) of the PN ligand observed for almost all allylpalladium complexes, when compared to those values found in the free ligand, indicate a chelate bonded ligand in solution, which is corroborated by conductivity experiments in CH_3OH (Section 2). The observation that the complexes with a chloride counter-ion are non-conducting in CH_2Cl_2 but conducting in CH_3OH is in accordance with the results obtained by Åkermark and co-workers on similar complexes [35], and is due to the formation of contact ion-pairs in CH_2Cl_2.

The ^1H and $^{13}C\{^1H\}$ NMR spectra of the allyl groups were assigned by comparison with literature values [36] and by making use of the observation that *trans* $^{31}P–^1H$ coupling constants are generally larger than *cis* $^{31}P–^1H$ coupling constants [37].

^1H and $^{31}P\{^1H\}$ NMR data at 213 K (Table 6) show that complex **9a** occurs in two isomeric forms in about a 1:1 ratio.

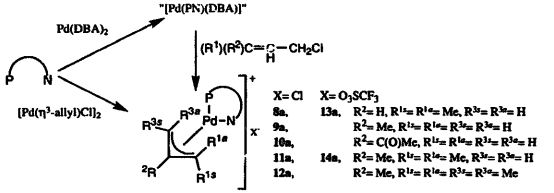

Scheme 2. Numbering of the η³-allyl complexes.

Table 6
^{31}P and relevant ^{1}H NMR of the η^3-allyl complexes **8a–14a**, measured in $CDCl_3$

Complex	X	T (K)	^{31}P	Y-Z	H^{1g}	R^{1s}	R^{1a}	R^{2}	R^{3s}	R^{3a}
 (8a)	Cl	298	24.5	P-N	8.64[b]	4.90[b] (H)	2.65[dd] [6.7]{9.2}(H)	5.13[bt] {9.2}(H)	1.76[d] [6.0](Me)	1.30[d] [4.1](Me)
		213	23.0 (19%)		[b]	[b]	[b]	[b]	[b]	[b]
			22.2 (19%)		[b]	[b]	[b]	[b]	[b]	[b]
			20.2 (62%)		[b]	[b]	[b]	[b]	[b]	[b]
 (9a)	Cl	298	25.2	P-N	9.40[s]	3.99[b] (H)	3.17[b] (H)	1.95[s] (Me)	3.99[b] (H)	3.17[b] (H)
		213	26.2 (42%)	P-N	9.12[s]	3.77[s] (H)	2.29[s] (H)	1.34[s] (Me)	obs.	2.85[d] [9.6](H)
			25.9 (58%)	P-N	9.45[s]	3.98[s] (H)	2.88[s] (Me)	0.95[s] (Me)	5.20[d] [6.3](H)	3.20[d] [9.6](H)
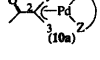 (10a)	Cl	298	28.8[b]	P-N	8.59[b]	4.31[b] (H)	2.95[b] (H)	2.38[s] (Me)	4.31[b] (H)	2.95[b] (H)
		213	27.9 (48%)	P-N	[b]	[b]	[b]	[b]	[b]	[b]
			27.4 (52%)	P-N	[b]	[b]	[b]	[b]	[b]	[b]
 (11a)	Cl	298	21.2[b]	–	9.07[b]	4.26[b] (H)	2.81[b] (H)	1.77[b] (Me)	1.77[b] (Me)	1.22[b] (Me)
		213	27.9 (50%)	N-P	9.29[s]	3.88[d] [5.4](H)	3.40[d] [9.9](H)	1.71[s] (Me)	1.64[s] (Me)	1.09[s] (Me)
			27.7 (50%)	N-P	8.94[s]	3.99[d] [6.7](H)	3.49[d] [10.1](H)	1.80[s] (Me)	1.67[s] (Me)	0.82[s] (Me)
 (12a)	Cl	298	21.5[b]	P-N	9.01[b]	1.89[b] (Me)	1.21[b] (Me)	1.90[b] (Me)	1.89[b] (Me)	1.21[b] (Me)
		213	25.6 (36%)	P-N	[b]	[b]	[b]	[b]	[b]	[b]
			22.9 (34%)	P-N	[b]	[b]	[b]	[b]	[b]	[b]
			21.1 (30%)	–	[b]	[b]	[b]	[b]	[b]	[b]
 (13a)	OTf	298	29.1 (58%)	P-N	8.38[b]	3.32[d] {10.6}(H)	2.72[dd] [3.2]{9.7}(H)	5.14[b] (H)	1.90[d] [10.6](Me)	1.49[d] [6.2](Me)
			23.5 (22%)	N-P	8.75[o]	4.15[dd] {7.8}[11.2](H)	3.38[dd] {3.8}[10.1](H)	5.0[dd] {3.8}{7.8}(H)	1.62[s] (Me)	1.62[s] (Me)
			22.9 (20%)	N-P	8.69[b]	4.00[bd] [7.0](H)	3.14[d] [12.6](H)	5.25[b] (H)	1.36[s] (Me)	1.18[s] (Me)
 (14a)	OTf	298	28.8 (14%)	P-N	8.18[b]	3.83[b] (H)	2.84[d] [3.3](H)	1.58[s] (Me)	1.79[d] [8.3](Me)	1.51[d] [6.2](Me)
			28.1 (19%)	P-N	8.49[b]	3.71[b] (H)	2.94[d] [3.1](H)	1.62[s] (Me)	1.91[d] [7.1](Me)	1.48[b] (Me)
			24.2 (36%)	N-P	8.68[b]	4.01[d] [6.7](H)	3.57[d] [4.2](H)	1.75[s] (Me)	1.57[s] (Me)	0.90[s] (Me)
			23.6 (31%)	N-P	8.70[b]	4.10[d] [7.1](H)	3.53[d] [3.7](H)	1.99[s] (Me)	1.67[s] (Me)	0.84[s] (Me)

[ ] = $^{3}J_{P-H}$, { } = $^{3}J_{H-H}$, [obs] obscured, [s] singlet, [b] broad, [d] doublet, [dd] double doublet, [bd] broad doublet, [bt] broad triplet.

The only explanation for the existence of two isomers lies in the fact that the Me substituent on the C^2 carbon may point up and down with respect to the chiral ligand backbone of the PN ligand [38]. At 298 K the signals of the two inequivalent *syn*-protons have coalesced (3.99 ppm) as is also the case for the *anti*-proton signals (3.17 ppm), while only one $^{31}P\{^1H\}$ signal is observed. This indicates the rapid interconversion of the two isomers together with a left–right (η^3–η^3) movement of the allyl group. This fluxional behavior may be explained by a Berry pseudo-rotational movement in a five-coordinate intermediate [36a,39,40], as the Cl^- ion will be close to the Pd(II) atom (vide supra). Alternatively one might think of an intermediate with an η^1-bonded PN ligand analogous to the mechanism proposed by Bäckvall and coworkers [41] for complexes [Pd(η^3-allyl)(NN)]OTf. This intermediate may in our case be stabilized by the Cl^- anion. We should note that neither the ^1H nor the $^{31}P\{^1H\}$ signals coalesce to the weighted mean of the low temperature signals (Table 6), which indicates that at 298 K one of the isomers becomes preponderant. When considering the complexes **10a** and **12a** which both also contain symmetrically substituted allyl groups, obviously analogous fluxional movements occur at 298 K.

The $^{31}P\{^1H\}$ NMR spectra of **10a** at 213 K show the presence of two isomers in about a 1:1 ratio, while the situation for **12a** is more complicated as three $^{31}P\{^1H\}$ signals are observed. It is tentatively assumed that the signals at 25.6 and 22.9 ppm of **12a** (Table 6) in about a 1:1 ratio are analogous to the low temperature isomers of **9a**. The $^{31}P\{^1H\}$ signal at 21.1 ppm (30%) cannot be assigned properly, but may be due to an η^1-PN (P-)bonded isomer [42], which is not unreasonable when the expected strong steric hindrance of the four methyl groups with the PN ligand is considered. No further comments will be made with regards to **10a** and **12a**, as the ^1H NMR spectra show broad signals at 213 K.

Now attention is paid to complexes **8a**, **11a**, **13a** and **14a** (Table 6) which all contain two methyl substituents at one end of the allyl group. Firstly, the observation that fluxional behavior occurs for the chloride complexes and not for the triflate ones, strongly indicates the involvement of Cl^- in the dynamic behavior of the intermediates, as has been pointed out above. Since **14a** shows all four expected isomers, the discussion of the allylpalladium complexes is started with this complex. From the ^{31}P–^1H coupling constants, the species occurring in concentrations of 36% and 31% is tentatively assigned to the up and down isomers of the complex which contains the P atom *cis* to the CMe_2 end of the allyl group (N-P isomer: $^3J_{P-H}1s = 7.1$ and 6.7 Hz; $^3J_{P-H}1a = 3.7$ and 4.2 Hz) and the less abundant isomers (14% and 19%) to the up and down isomers of the complex with the P atom *trans* to the CMe_2 group (P-N isomer: $^3J_{P-Me}3s = 8.3$ and 7.1 Hz; $^3J_{P-Me}3a = 6.2$ Hz). In the case of **13a**, however, three isomers are observed. Interestingly, the ^{31}P–$^1H^{1s}$ (11.2 and 7.0 Hz) and ^{31}P–$^1H^{1a}$ (10.1 and 12.6 Hz) coupling constants strongly indicate that the two less abundant isomers (20% and 22%) are the up and down forms of the compound with the P atom *cis* to the CMe_2 group (N-P isomer), while the most abundant isomer (58%) represents one form (up or down) of the complex with the P atom *trans* to the CMe_2 moiety (P-N isomer: $^3J_{P-Me}3s = 10.6$ Hz; $^3J_{P-Me}3a = 6.2$ Hz). If these assignments are correct, it is interesting that the simple substitution of an H atom on the 2-position (**13a**) by a methyl group (**14a**) reverses the relative concentrations of N-P and P-N bonded isomers. Electronic factors predict the P-N isomer to be the predominant isomer present in solution [36e], while CPK models show a selective steric interaction of $C(21)H_3$ of the ligand with the *anti* oriented allylic methyl group in the P-N isomer, similar to the effect found by Åkermark et al. using a methyl substituted phenanthroline ligand [43].

Little will be said about **8a** as proper low temperature ^1H NMR spectra are lacking, but it should be noted that, on the basis of $^{31}P\{^1H\}$ NMR, three isomers are present at low temperature, which coalesce at 298 K. From coupling constants it appears that at 298 K the P atom is *trans* to the CMe_2 group. Fortunately the ^1H NMR spectra of **11a** at 213 K could be measured, which shows the presence of only two isomers in about a 1:1 ratio. From the ^1H NMR data it is clear that these represent the up and down isomers of the complex with the P atom *cis* to the CMe_2 moiety (N-P isomer), while P-N bonded isomers which are present for the triflate complex **14a**, albeit as the minor isomers, do not occur in the case of the chloride complex **11a**. This again demonstrates that the Cl^- anion exerts a strong influence on the type of isomer (N-P versus P-N) formed and must therefore be close in space to the Pd atom. With respect to **11a** it is interesting that at 298 K the ^1H NMR signals lack $^{31}P\{^1H\}$ coupling, which may indicate intermolecular exchange of the PN ligand. Also the $^{31}P\{^1H\}$ and ^1H NMR chemical shifts at 298 K of **11a** are quite different when compared to the spectra at 213 K, which indicate the presence of a different isomeric form (or forms) at 298 K on which we are not able to comment.

3.3. Reactivity of the complexes

3.3.1. [MX(C(O)Me)(L)] (M = Pd, X = Cl, Br, I, OTf; M = Pt, X = Cl, I, OTf)

Insertion of CO into the methylmetal bond of **4a–7a** and **4b–7b** occurred by pressurizing an evacuated reaction vessel or by bubbling CO through a solution for a prolonged period of about an hour. The acyl products (**15**, **16** and **17** in Scheme 3) are unstable under both CO and N_2 atmosphere, with formation of colloidal palladium or platinum. The ionic palladium (**7a**) and platinum (**7b**) complexes in $CDCl_3$ show, under a CO atmosphere, immediate formation of **18a** and **18b**, respectively, which is accompanied by the formation of colloidal palladium or platinum (Scheme 3).

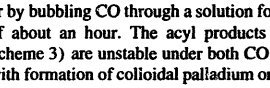

Scheme 3. Numbering of the acyl complexes.

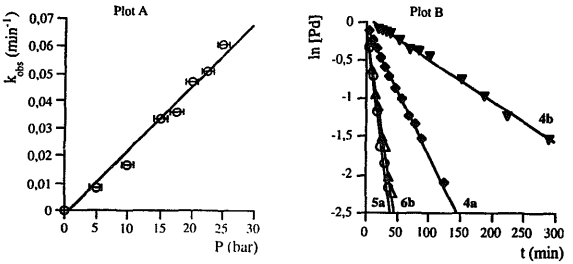

Fig. 3. CO insertion data ($CDCl_3$). Plot A: insertion rate k_{obs} (min^{-1}), vs. pressure of CO for **4a**, measured at 293 K. Plot B: CO insertion data for **4a**, **4b**, **5a** and **6b**. The logarithmic decrease of the starting complexes vs. time (min) when 10 bar CO is applied, measured at 293 K. The insertion rates (k_{obs}) were calculated using $\ln\{[(C(t)]/(C(0)]\} = -kt$.

The coordination mode of the PN ligand in the acyl complexes is comparable to that of the corresponding methyl compounds, as shown by the upfield shifts of the $^{31}P\{^1H\}$ resonance signals when compared to the alkyl complexes ($\Delta\delta = 18$ ppm for Pd, $\Delta\delta = 10$ ppm for Pt complexes) and the upfield shift of the imine proton in ^1H NMR (7.93–7.70 ppm) relative to the free ligand value of 9.11 ppm (Table 4).

Monitoring the insertion reaction of CO into the methyl-metal bond of the neutral alkyl complexes (**4a–6a**, **4b** and **6b**), by $^{31}P\{^1H\}$ and ^1H NMR, shows that the acetyl product is slowly formed, while no intermediates are observed.

Investigation of the insertion of CO into the methylpalladium bond of **4a** with different pressures of CO (5–25 bar) of which only one result (10 bar CO) is presented in Fig. 3 (plot B), shows that the insertion is first order in palladium and first order in CO (Fig. 3, plot A). The reactivity using 10 bar of CO, expressed by the half-lives of the alkyl complexes (42 ± 3 min (**4a**); 12 ± 2 min (**5a**); <2 min (**6a**); <2 min (**7a**); 127 ± 4 min (**4b**); 14 ± 1 min (**6b**); 152 min (**7b**)), increases on going from chloride to iodide. The palladium complexes react notably faster than the corresponding platinum compounds (Fig. 3, plot B), due to the higher stability of the latter complexes.

The ionic methylpalladium complex (**7a**^{s}: Scheme 4), which contains a non-coordinating OTf anion, as indicated by the ^{19}F NMR resonance shift of -78.4 ppm, dissolved in CD_3OD shows some intermediates during the CO insertion

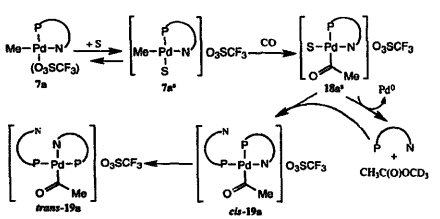

Scheme 4. Insertion of CO into the Pd–Me bond of [Pd(Me)(L)]OTf (**7a**) dissolved in CD_3OD.

reaction which were not observed when this reaction was carried out in $CDCl_3$.

The $^{31}P\{^1H\}$ NMR resonance signal of **7a** at 41.0 ppm (CD_3OD) disappears upon CO pressure with the formation of a singlet at 24.3 ppm, which is accompanied by the disappearance of the Pd–Me resonance in ^1H NMR, indicating the formation of a [Pd(C(O)Me)(η^2-PN)]$^+$ complex (**18a**^{s}: Scheme 4).

Subsequently this $^{31}P\{^1H\}$ singlet at 24.3 ppm slowly disappears with the formation of two doublets at 51.8 and 18.2 ppm ($^2J_{P-P} = 24$ Hz), indicating two inequivalent phosphines bonded to the palladium center in a *cis* orientation [44]. ^1H NMR shows a shift of the acyl resonance to 1.12 ppm and a broad imine doublet at 8.68 ppm ($^4J_{P-H} = 11.6$ Hz). During this reaction a compound is formed which exhibits a $^{13}C\{^1H\}$ resonance at 173.2 ppm and a ^1H singlet at 2.03 ppm, indicating the formation of $CH_3C(O)OCD_3$ and a Pd–H species [45,46]. Since this reaction is accompanied by the formation of a large amount of colloidal palladium (approximately 50%) while no free ligand is observed, the two doublets indicate the presence of a complex in which the liberated ligand is also coordinating to the [Pd(C(O)Me)(η^2-PN)]$^+$ complex, thus forming *cis*-[Pd(C(O)Me)(η^1-PN)(η^2-PN)]$^+$ (*cis*-**19a**). Unfortunately we were not able to elucidate the structure of this product properly since no ^1H line sharpening (or splitting) was observed in the 213–313 K temperature range.

Finally, these two $^{31}P\{^1H\}$ NMR doublets disappear slowly, with the formation of a $^{31}P\{^1H\}$ singlet at 33.1 ppm, while the ^1H acyl resonance at 1.29 ppm and the broad imine doublet at 9.24 ppm ($^4J_{P-H} = 13.9$ Hz), indicate an intramolecular transformation of the *cis* product to *trans*-[Pd(C(O)Me)(η^1-PN)(η^2-PN)]$^+$ (*trans*-**19a**). Low temperature NMR (213 K) did not show splitting of the $^{31}P\{^1H\}$ or the ^1H imine or H^{21} resonances, indicating a fast η^1–η^2 PN exchange.

In order to study the geometry of the intermediates observed during the reaction of **7a** with CO in CD_3OD, free ligand was added to a solution of **7a** (CD_3OD), which imme-

diately resulted in a broad $^{31}P\{^1H\}$ NMR resonance signal at 26.9 ppm, while the ^1H NMR spectra at room temperature show upfield shifts of H^{19} (8.73 ppm), H^{20} (1.15 ppm) and H^{21} (4.10 ppm). The $^{31}P\{^1H\}$ and ^1H shifts indicate the formation of *trans*-[Pd(Me)(η^2-PN)(η^1-PN)](O_3SCF_3), which did not show splitting of the ^1H imine or $^{31}P\{^1H\}$ signals at 213 K, indicating again a fast η^1–η^2 PN exchange.

The ionic platinum complex **7b**, also having a non-coordinating OTf anion (^{19}F NMR: −78.8 ppm), however, does not show the formation of intermediates in which two ligands are bonded to the metal center. Instead, it has been found that upon pressurizing **7b** under CO a complex is formed which exhibits a $^{31}P\{^1H\}$ NMR resonance signal at 23.5 ppm ($^1J_{Pt-P}$ = 3470 Hz) and a ^1H Pt–Me resonance at 0.53 ppm ($^3J_{Pt-H}$ = 72.3 Hz; $^4J_{P-H}$ = 5.9 Hz). This $^1J_{Pt-P}$ coupling is a typical value found for compounds in which a CO ligand is positioned *trans* to a phosphorus donor [47], which is also in accord with the CO stretch of 2109 cm^{-1}. Therefore we assign these data to an intermediate [Pt(Me)(CO)(L)]-(O_3SCF_3). The $^{31}P\{^1H\}$ resonance at 23.5 ppm subsequently disappears slowly with the formation of a $^{31}P\{^1H\}$ signal at 12.4 ppm with a $^1J_{Pt-P}$ of 3965 Hz, indicating a CO ligand *trans* to phosphorus [48]. This is accompanied by the formation of an ^1H acetyl resonance at 2.02 ppm, indicating therefore the formation of [Pt(C(O)Me)(CO)(L)]-(O_3SCF_3). The acyl product decarbonylated upon releasing the CO pressure to form the [Pt(Me)(CO)(L)](O_3SCF_3) intermediate. Clearly a ligand, in this case CO, coordinated *cis* to the acyl group is needed to stabilize the Pt-acyl product, as is more frequently observed [1b,5]

4. Discussion

There are some aspects of this work which merit some more attention. Firstly, when discussing the insertion of CO into the metal–methyl bond of [MX(Me)(PN)] (M = Pd, Pt; X = Cl, Br, I, OTf) affording [MX(C(O)Me)(PN)] (M = Pd, Pt; X = Cl, Br, I, OTf) respectively, it is noted that, as found before [1b], the methyl group in the starting compound and the acetyl group in the product are *cis* to the P atom, which is the atom with the highest *trans* influence [49]. Furthermore, the Pt complexes show lower insertion rates than the Pd compounds, as the Pt complexes are kinetically more robust. In earlier work it was reported [1b] that, provided that the PN ligand remains bidentate bonded during the insertion, the reaction may proceed via two routes (Scheme 5).

The reaction via route I has to go via an extra rearrangement barrier before insertion or via a large kinetic barrier in the migration step (route II), as it is known that insertion preferably occurs when the Me group is *trans* to P. In the case of Pt complexes it was demonstrated [1b] for both rigid and flexible PN ligands that the insertion took place via intermediates containing an η^1-PN (P-)bonded ligand, thereby indicating that the insertion step is rate determining. Since the complexes discussed in this article show a relatively slow insertion we were able to carry out some kinetic measurements (Fig. 3) which demonstrate that the reaction is first order in CO and first order in the complex, while no evidence was found for a CO independent pathway. This means that either the association step of CO to the starting complex or the insertion step is rate determining. Although no intermediates were observed for the neutral Pd and Pt systems, we tentatively suggest that the insertion step is rate determining, in view of earlier results [1b]. The observation that the rates increase in the order Cl < Br < I does not distinguish between the two possibilities as both steps are expected to be faster in this order. It has been noted before that alkenes which insert in the acyl metal bond of complexes [Pd(R)(Y)(L-L)] (L-L = NN or PP) do not insert at all when L-L is a PN ligand. Also for the complexes discussed in this chapter insertion of alkenes is not observed, while only allenes insert, but very slow indeed (60% conversion after two weeks). Since the structural and dynamic features of η^3-allyl palladium complexes containing chiral NS [34] and PN ligands are also of interest, it was decided to prepare complexes [Pd(η^3-allyl)(PN)]X (X = Cl, OTf) by different routes (see Sections 2 and 3).

On the basis of the NMR results (Table 6) a number of questions may be addressed: (i) why is in virtually all cases the ratio between the up and down forms approximately the same; (ii) which factors determine the formation of N-P and P-N bonded isomers in the case of the complexes containing asymmetrically substituted η^3-bonded allyl groups, i.e. in this study a CMe_2 moiety on one end of the allyl group. First of all it is known that for electronic reasons the atoms with the

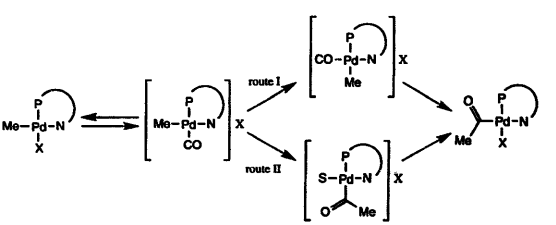

Scheme 5. Two possible routes for the CO insertion reaction.

largest *trans* influence prefer generally to be *trans* to the C atom containing alkyl substituents, so we would expect the P atom to be *trans* to the CMe_2 group [36e]. Steric factors obviously play an important role and to answer the questions above we made use of simple CPK models with the configuration of the *R*-(±)-PN ligand based on the molecular structures reported in this paper. It should be realized that only very qualitative conclusions may be drawn. It appears first of all obvious that the substituent R^2 on the central carbon atom of the allyl group does not come into close contact with any part of the bidentate bonded ligand, which explains the 1:1 ratio of the up and down forms of virtually all isomers investigated, i.e. of the chloride complexes at low temperatures and of the triflate complex **14a** at 298 K. Not clear at all is why for **13a** only one form (up or down) for the P-N bonded isomers, which is expected to give a faster η^3–η^1–η^3 exchange than the N-P bonded isomers, is observed (Table 6).

When the question whether P-N or N-P bonded isomers are formed, if one end of the allyl group contains a CMe_2 moiety, is considered, the answer lies in the observation that the CMe_2 group is sterically much more hindered by the N–CH(Me)(Ph) function than by the two flat phenyl groups of the PPh_2 moiety [40]. So, for complexes **11a** and **14a** the steric influence dominates the electronic factor while the reverse is the case for **13a**. Since we are dealing with relatively small energy differences it is not useful to discuss this point further.

Interesting is to compare the chloride complex **11a** with the triflate analogue **14a**, since in the case of **11a** (at 213 K) one observes only the up and down forms of the N-P bonded isomer while in the case of **14a** also about 30% of the up and down forms of the P-N bonded isomer is present. As the chloride complex **11a** is in CH_2Cl_2 a non-conductor in contrast to **14a**, it is clear that the Cl^- anion must be close to the Pd atom (contact ion-pair), which should clearly have an influence on the configuration of the ligand and of the allyl group. The CPK models could not give us a definite answer to this problem and again we should recall that energy differences will be small.

Finally attention is paid to the point that within each isomeric form (P-N bonded or N-P bonded) the up and down forms can only be interconverted by an η^3–η^1–η^3 movement provided that the ligand remains bidentate bonded (Scheme 6). Since no coalescence of either the CH_2 or the CMe_2 protons is observed at room temperature, this isomerization path is rather unlikely for the P-N bonded isomer at room temperature. However, a fast η^3–η^1–η^3 isomerization of the N-P bonded isomer cannot be excluded. It is clear that the up form of the P-N bonded isomer can only be converted into the down form of the N-P bonded isomer (and vice versa) by an η^3–η^3 rearrangement which may proceed via Berry pseudo-rotations in a five-coordinate intermediate (Scheme 6, route A) [36a,38,39].

However, if one assumes a mechanism as recently proposed by Pregosin and co-workers [50] and Bäckvall et al.

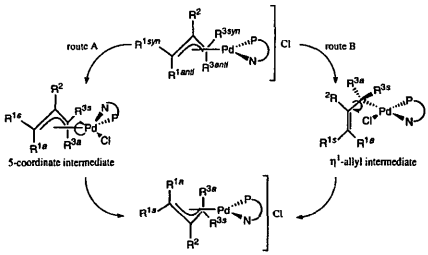

Scheme 6. The rotational isomers of the η^3-allyl complexes and their possible interconversion pathways.

[41] which involves intermediates with monodentate bonded nitrogen ligands, i.e. in this case an η^1-PN (P-) bonded ligand, it is much more easy to interconvert all isomers. Unfortunately, none of these complexes with the asymmetrically substituted allyl group studied was found to be suitable for more detailed investigations of dynamic behavior.

5. Supplementary material

Further details of the structure determinations, including atomic coordinates, bond lengths and angles, and thermal parameters (15 pages for **1a**, 16 pages for **3b**, 25 pages for **4a**) are available from the authors on request.

Acknowledgements

This work was supported by the Netherlands Foundation of Chemical Research (SON) with financial aid from the Netherlands Organisation for Scientific Research (NWO) (A.L.S.) and by the award of a postdoctoral fellowship under the EC Human Capital and Mobility initiative (M.T.L.). Thanks are also due to J.-M. Ernsting for support in collecting the NMR data and Dr C.J. Elsevier for his interest and suggestions.

References

[1] (a) P.G.C.M. Dekker, C.J. Elsevier, K. Vrieze and P.W.N.M. van Leeuwen, *Organometallics, 11* (1992) 1598; (b) P.G.C.M. Dekker, A. Buijs, C.J. Elsevier, K. Vrieze, P.W.N.M. van Leeuwen, W. Smeets, A.L. Spek, Y.F. Wang and C. Stam, *Organometallics, 11* (1992) 1937.

[2] (a) R. van Asselt, C.J. Elsevier, W.J.J. Smeets and A.L. Spek, *Inorg. Chem., 33* (1994) 1521; (b) R. van Asselt, C.J. Elsevier, W.J.J. Smeets, A.L. Spek and R. Benedix, *Recl. Trav. Chim. Pays-Bas, 113* (1994) 88; (c) R.E. Rülke, M. Han, C.J. Elsevier, K. Vrieze, P.W.N.M. van Leeuwen, C.F. Roobeek, M.C. Zoutberg, Y.F. Wang and C.H. Stam, *Inorg. Chim. Acta, 169* (1990) 5.

[3] I. Toth and C.J. Elsevier, *J. Am. Chem. Soc., 115* (1993) 10388.

[4] R. van Asselt, E.C.G. Gielens, R.E. Rülke and C.J. Elsevier, *J. Chem. Soc., Chem. Commun.*, (1993) 1203.

[5] P.W.N.M. van Leeuwen, C. Roobeek and H. van der Heyden, *J. Am. Chem. Soc., 116* (1994) 12117.
[6] R.E. Rülke, V.E. Kaasjager, D. Kliphuis, C.J. Elsevier, P.W.N.M. van Leeuwen, K. Vrieze and K. Goubitz, *Organometallics*, in press.
[7] (a) E.W. Abel, N.J. Long, K.G. Orrell, A.G. Osborne, H.M. Pain and V. Sik, *J. Chem. Soc., Chem. Commun.*, (1992) 303; (b) E.W. Abel, V.S. Dimitrov, N.J. Long, K.G. Orrell, A.G. Osborne, V. Sik, M.B. Hursthouse and M.A. Mazid, *J. Chem. Soc., Dalton Trans.*, (1993) 291; (c) E.C. Constable and A.M.W. Cargill Thompson, *Inorg. Chim. Acta, 233* (1994) 177; (d) E.C. Constable, A.J. Edwards, M.J. Hannon and P.R. Raithby, *J. Chem. Soc., Chem. Commun.*, (1994) 1991.
[8] R.E. Rülke, J.M. Ernsting, A.L. Spek, C.J. Elsevier, P.W.N.M. van Leeuwen and K. Vrieze, *Inorg. Chem., 32* (1993) 5769.
[9] M.F. Rettig and P.M. Maitlis, *Inorg. Synth., 17* (1977) 134.
[10] T.B. Rauchfuss and D.A. Wrobleski, *Inorg. Synth., 21* (1982) 175.
[11] C.J. Elsevier, *J. Mol. Catal., 92* (1994) 285.
[12] J.L. de Boer and A.J.M. Duisenberg, *Acta Crystallogr., Sect. A, 40* (1984) C410.
[13] A.L. Spek, *J. Appl. Crystallogr., 21* (1988) 578.
[14] L.E. McCandlish, G.H. Stout and L.C. Andrews, *Acta Crystallogr., Sect. A, 31* (1975) 245.
[15] N. Walker and D. Stuart, *Acta Crystallogr., Sect. A, 39* (1983) 158.
[16] P.T. Beurskens, G. Admiraal, G. Beurskens, W.P. Bosman, S. García-Granda, R.O. Gould, J.M.M. Smits and C. Smykalla, The DIRDIF program system, *Tech. Rep.*, Crystallography Laboratory, University of Nijmegen, Netherlands, 1992.
[17] G.M. Sheldrick, *SHELX86*, program for crystal structure determination, University of Göttingen, Germany, 1986.
[18] G.M. Sheldrick, *SHELX76*, program for crystal structure determination, University of Cambridge, UK, 1976.
[19] G.M. Sheldrick, *SHELXL-93*, program for crystal structure refinement, University of Göttingen, Germany, 1993.
[20] H.D. Flack, *Acta Crystallogr., Sect. A, 39* (1983) 876.
[21] A.J.C. Wilson (ed.), *International Tables for Crystallography*, Vol. C. Kluwer, Dordrecht, Netherlands, 1992.
[22] D.T. Cromer and J.B. Mann, *Acta Crystallogr., Sect. A, 24* (1986) 321.
[23] D.T. Cromer and D. Liberman, *J. Chem. Phys., 53* (1970) 1891.
[24] (a) A.L. Spek, *Acta Crystallogr., Sect. A, 46* (1990) C34; (b) *PLUTON*, molecular graphics program, Utrecht University, Netherlands, 1995.
[25] A. Lavery and S.M. Nelson, *J. Chem. Soc., Dalton Trans.*, (1984) 615.
[26] H.A. Ankersmit, N. Veldman, A.L. Spek, K. Eriksen, K. Goubitz, K. Vrieze and G. van Koten, *Inorg. Chim. Acta, 252* (1996) 203.
[27] J.C. Jeffery, T.B. Rauchfuss and P.A. Tucker, *Inorg. Chem., 19* (1980) 3306.
[28] (a) F. Cecconi, C.A. Ghilardi, S. Midollini, S. Moneti, A. Orlandini and G. Scapacci, *J. Chem. Soc., Dalton Trans.*, (1989) 211; (b) S. Perera, B.L. Shaw and M. Thornton Pett, *J. Chem. Soc., Dalton Trans.*, (1992) 999; (c) K. Tani, M. Yabuta, S. Nakamura and T. Yamagata, *J. Chem. Soc., Dalton Trans.*, (1993) 2781; (d) R.E. Rülke, P.W.N.M. van Leeuwen and K. Vrieze, to be published; (e) B. Jedlicka, N. Veldman, A.L. Spek and W. Weissensteiner, to be published; (f) D.P. Arnold, M.A. Bennet, M.S. Bilton and G.B. Robertson, *J. Chem. Soc., Chem. Commun.*, (1982) 115; (g) S. Fallis, G. Anderson and N.P. Rath, *Organometallics, 10* (1991) 3180; (h) F.P. Fanizzi, F.P. Intini, L. Maresca, G. Natile, M. Lanfranchi and A. Tiripicchio, *J. Chem. Soc., Dalton Trans.*, (1991) 1007.
[29] J.G. Verkade and J.A. Mosbo, in J.G. Verkade and L.D. Quin (eds.), *Phosphorus-31 NMR Spectroscopy in Stereochemical Analysis*, Vol. 8, VCH, Deerfield Beach, FL, 1987, p. 438.
[30] T.G. Appleton, H.C. Clark and L.E. Manzer, *Coord. Chem. Rev., 10* (1973) 335.
[31] G.C. van Stein, G. van Koten, K. Vrieze, C. Brevard and A.L. Spek, *J. Am. Chem. Soc., 106* (1984) 4486.
[32] J.H. Groen, C.J. Elsevier, K. Vrieze, W.J.J. Smeets and A.L. Spek, to be published.
[33] (a) R.E. Rülke, D. Kliphuis, C.J. Elsevier, J. Fraanje, K. Goubitz, P.W.N.M. van Leeuwen and K. Vrieze, *J. Chem. Soc., Chem. Commun.*, (1994) 1817; (b) J.P.G. Delis, P.W.N.M. van Leeuwen and K. Vrieze, to be published.
[34] H.A. Ankersmit, N. Veldman, A.L. Spek, K. Eriksen, K. Goubitz, K. Vrieze and G. van Koten, to be published.
[35] M.P.T. Sjörgen, S. Hansson, P-O. Norrby, B. Åkermark, M.E. Cucciolito and A. Vitagliano, *Organometallics, 11* (1992) 3954.
[36] (a) K. Vrieze, P. Cossee, A.P. Praat and C.W. Hilbers, *J. Organomet. Chem., 11* (1968) 353; (b) R.P. Hughes and J. Powell, *J. Organomet. Chem., 60* (1973) 409; (c) Y. Senda, H. Suda, J. Ishiyama, S. Imaizumi, A. Kasahara, T. Izumi and T. Kato, *Bull. Chem. Jpn., 50* (1977) 1608; (d) B.M. Trost, P.E. Strege, L. Weber, T.J. Fullerton and T.J. Dietsche, *J. Am. Chem. Soc., 100* (1978) 3407; (e) B. Åkermark, B. Krakenberger, S. Hansson and A. Vitagliano, *Organometallics, 6* (1987) 620; (f) B. Crociani, S. Antonaroli, F. Di Bianca and A. Fontana, *J. Organomet. Chem., 450* (1993) 21.
[37] P.S. Pregosin and R.W. Kunz, in P. Diehl, E. Fluck and R. Kosfeld (eds.), *NMR Basic Principles and Progress*, Springer, Heidelberg, 1979, p. 28.
[38] C. Breutel, P.S. Pregosin, R. Salzman and A. Togni, *J. Am. Chem. Soc., 116* (1994) 4067.
[39] K. Vrieze, P. Cossee and A.P. Praat, *Recl. Trav. Chim. Pays-Bas, 86* (1967) 769.
[40] S. Hansson, P-O. Norrby, M.P.T. Sjörgen, B. Åkermark, M.E. Cucciolito, F. Giordano and A. Vitagliano, *Organometallics, 12* (1993) 4940.
[41] A. Gogoll, J. Örnebro, H. Grennberg and J.E. Bäckvall, *J. Am. Chem. Soc., 116* (1994) 3631.
[42] (a) F.A. Cotton, J.W. Faller and A. Musco, *Inorg. Chem., 6* (1967) 179; (b) J. Powell and B.L. Shaw, *J. Chem. Soc. A*, (1967) 1839; (c) H. Kurosawa, H. Kajimaru, S. Ogoshi, H. Yoneda, K. Miki, N. Kasai, S. Murai and I. Ikeda, *J. Am. Chem. Soc., 114* (1992) 8417.
[43] B. Åkermark, S. Hansson and A. Vitagliano, *J. Am. Chem. Soc., 112* (1990) 4587.
[44] M.A. Bennet, D.E. Berry and K.A. Beveridge, *Inorg. Chem., 29* (1990) 4148.
[45] (a) C. Pisano, G. Consiglio, A. Sironi and M. Moret, *J. Chem. Soc., Chem. Commun.*, (1991) 421; (b) M. Barsacchi, G. Consiglio, L. Medici, G. Petrucci and U.W. Suter, *Angew. Chem., Int. Ed. Engl., 30* (1991) 989; (c) C. Pisano, A. Mezetti and G. Consiglio, *Organometallics, 11* (1992) 20.
[46] (a) D. Milstein, *Organometallics, 1* (1982) 888; (b) C. Pisano, A. Mezzetti and G. Consiglio, *Organometallics, 11* (1992) 20.
[47] (a) G.K. Anderson and R.J. Cross, *J. Chem. Soc., Dalton Trans.*, (1976) 1246; (b) T.G. Appleton and M.A. Bennet, *Inorg. Chem., 17* (1978) 738; (c) G.K. Anderson and R.J. Cross, *J. Chem. Soc., Dalton Trans.*, (1980) 1434.
[48] (a) A. Albinati, U. von Gunten, P.S. Pregosin and H.J. Ruegg, *J. Organomet. Chem., 295* (1985) 239; (b) P. van Leeuwen, C.F. Roobeek, J.H.G. Frijns and A.G. Orpen, *Organometallics, 9* (1990) 1211.
[49] (a) S. Sakaki, K. Kitaura, K. Morokuma and K. Ohkubo, *J. Am. Chem. Soc., 105* (1983) 2280; (b) N. Koga and K. Morokuma, *J. Am. Chem. Soc., 107* (1985) 7230; (c) *108* (1986) 6136.
[50] A. Albinati, R.W. Kunz, J. Christian, C.J. Ammann and P.S. Pregosin, *Organometallics, 10* (1991) 1800.